Journal of Physics:
Conference Series

PURPOSE-LED
PUBLISHING™

PAPER • OPEN ACCESS

Molecular Dynamics Insights into the Role of Sulfur in Asphaltene Solubility

To cite this article: Rena A. Jafarova *et al* 2026 *J. Phys.: Conf. Ser.* **3290** 012007

View the article online for updates and enhancements.

Enabling Electrochemistry
Inside and Outside the Lab

PalmSens

Discover our diverse range of Potentiostats engineered
to support your research wherever it takes you

- Intuitive software for Windows and Android
- Proven in over 4000 scientific publications
- Single-channel and multi-channel
- Benchtop, portable and wearable

Discover More



This content was downloaded from IP address 193.140.144.1 on 28/11/2026 at 20:19

Journal of Physics: Conference Series **3290** (2026) 012007 doi:10.1088/1742-6596/3290/1/012007

MOLECULAR DYNAMICS INSIGHTS INTO THE ROLE OF SULFUR IN ASPHALTENE SOLUBILITY

Rena A. Jafarova[1], Ulviyya J. Yolchuyeva[*1,2,3], Gunay A. Hajiyeva[1,2], Ayaz M. Mammadov[1,4], Nazli A. Mehdiyeva[1,2], Fargana Alizadeh[1,5], Chimnaz G. Salmanova[1], Elfana N. Gasimova[6], Abdallah A. K. Algherbawi[7], Peri A. Muradova[8], Aytekin Sh. Aliyeva[1], Sabina Q. Eldarova[1], Murad Z. Bayramov[9], Elmar S. Samadov[10]

[1]Institute of Petrochemical Processes of Ministry of Science and Education Republic of Azerbaijan, Baku, Azerbaijan
[2]Department of Chemical Engineering, School of Engineering and Applied Science, Khazar University, Baku, Azerbaijan
[3]Azerbaijan University of Architecture and Construction, Baku, Azerbaijan
[4]Sumgayit State University, Department of Chemistry, Sumgayit, Azerbaijan
[5]GPOGC SRI, Azerbaijan State Oil and Industry University, Baku, Azerbaijan
[6]Department of Design, Azerbaijan State University of Economics, Baku, Azerbaijan
[7]Chemical Engineering Department, Faculty of Engineering, Sivas Cumhuriyet University, Sivas, Türkiye
[8]Institute of Chemistry, Ministry of Science and Education of Azerbaijan, Baku, Azerbaijan
[9]Baku Higher Oil School, Baku, Azerbaijan
[10]Institute of Geology and Geophysics, Ministry of Science and Education of the Republic of Azerbaijan, Baku, Azerbaijan

e-mail: u.jeyhunzade@gmail.com

Abstract
The solubility of asphaltenes is heavily dependent on several variables, with heteroatoms, especially sulfur (S), acting as a primary determinant. For this research, we constructed asphaltene models utilizing existing empirical findings and specific computational metrics, employing molecular dynamics (MD) simulations to quantify how S impacts solubility and clustering patterns. These simulations aimed to explore the role of S in altering asphaltene dynamics within typical oil-industry solvents. Findings indicate that the specific location of S within the asphaltene framework fundamentally shifts the molecule's polarity, interactions with other molecules, and overall dissolving properties. Notably, locating S on an aliphatic branch alters the molecules' clustering habits and dictates how well they scatter throughout the solvent. Ultimately, these observations deepen our comprehension of the underlying mechanisms driving asphaltene activity, offering a theoretical foundation to formulate better methods for mitigating aggregation and solid buildup across oil extraction, transport, and refining stages.
Keywords: asphaltene clustering, MD simulations, electrostatic energy, H-bonding, van der Waals energy.

1. Introduction

Content from this work may be used under the terms of the Creative Commons Attribution 4.0 licence. Any further distribution of this work must maintain attribution to the author(s) and the title of the work, journal citation and DOI.
Published under licence by IOP Publishing Ltd

Against the backdrop of surging global energy demand and the progressive depletion of conventional oil reservoirs, the hydrocarbon industry is increasingly shifting its focus toward resources situated within complex geological settings, specifically targeting unconventional assets [1-4]. Within this context, a critical hurdle for operators is inhibiting the solid dropout of asphaltenes across the recovery, pipeline transit, and upgrading phases of heavy, asphaltene-dense crudes [5, 6]. The tendency of these complex molecules to cluster and stabilize persistent multiphase emulsions severely hinders crude dehydration processes, ultimately driving up operational expenditures [7, 8].

Structurally, asphaltene fractions are highly heterogeneous mixtures predominantly formed by C and H, heavily interspersed with heteroatoms, namely N, O, and S, alongside metallic traces like V, Ni, and Fe [9, 10]. The inherent polarity introduced by these elemental inclusions governs the overall phase stability of the fluid, acting as a primary driver for the aggregation and ultimate deposition of these molecular species [11-13]. Contemporary analytical breakthroughs have further resolved these structural ambiguities; high-resolution atomic force microscopy, for instance, has successfully imaged isolated molecules, confirming that their aromatic cores largely conform to “island” or “continental” architectural motifs [14, 15].

The equilibrium phase distribution of asphaltenes in petroleum fluids is shaped by a matrix of variables, namely system pressure, temperature, solute concentration, and the specific characteristics of the solvent environment [16]. Specific elemental constituents, particularly S and O, alongside V-porphyrin complexes, act as primary catalysts for both clustering and phase separation events [17-19]. Conversely, the steric bulk introduced by aliphatic branches frequently serves to restrict these clustering tendencies. Resin fractions stabilize asphaltene molecules by maintaining them in a dispersed state; however, their removal disrupts colloidal stability and promotes asphaltene flocculation and precipitation over time [20-22].

To explore these effects with atomistic detail, computational modeling using the principles of molecular dynamics (MD) has established itself as a critical resource. This method enables the evaluation of intermolecular interactions as well as key system parameters such as temperature, pressure, and energy. Previous studies have used model asphaltene structures with similar aromatic cores to better elucidate aggregation mechanisms [23-25].

The position of heteroatoms within asphaltene molecules significantly affects aggregation behavior. In particular, the location of sulfur atoms can influence the π-electron system and intermolecular interactions, thereby affecting solubility and aggregation properties [26-28]. Consequently, the present study deploys MD simulations to evaluate the clustering dynamics of paired asphaltene structures, differentiated by the spatial placement of their disulfide linkages, across octane and xylene media. The primary objective is to elucidate how S constituents modulate these clustering tendencies across distinct solvent matrices.

2. Material and methods

The asphaltene sample No. 11858-06 was obtained in accordance with GOST [ГОСТ 11244-76] standards and used for the study. Cryoscopic analysis utilizing a naphthalene solvent established the mean molecular mass of the extracted fraction at 776.

The model structure of the asphaltene molecule, whose structure was established using spectroscopic methods, is presented in Figure 1. In the selected model molecule, the sulfur atom is located in an aliphatic side chain in the form of an –S-S– bridge (A). We utilized this specific molecular framework to probe the intermolecular forces and clustering dynamics characteristic of asphaltenes.

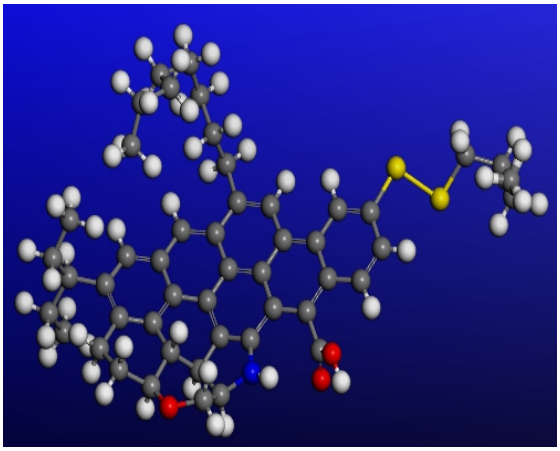

Figure 1. Visual representation of the chemical architecture and energy-minimized geometry for the target asphaltene structures.

To evaluate the dissolution characteristics of these asphaltene units, MD computational runs were executed via the Materials Studio 6.0 platform. The COMPASS force field was applied throughout all simulation stages [29, 30]. Prior to the simulations, geometrical optimization was carried out to obtain energetically stable structures and eliminate unstable interactions. All simulation trajectories incorporated periodic boundary conditions, using a time increment of 1 fs for the numerical integration.

A Nosé thermostat handled temperature control in the NVT ensemble, while pressure regulation was achieved using the Berendsen barostat in the NPT ensemble. These computational runs spanned a 300 ps timeframe, continuously maintained under standard conditions of 298 K and 1 atm.

Furthermore, to accurately capture solute-solvent dynamics, we generated an energy-minimized model of the respective solvent. The molecular architecture of this solvent species is portrayed as Figure 2.

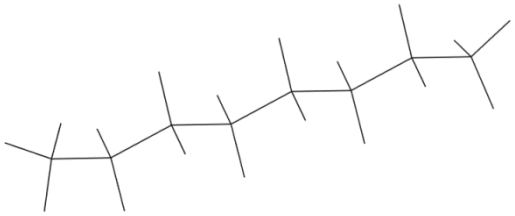

Figure 2. Geometry-optimized structure pertaining to the aliphatic solvent (octane) used in the simulations.

The target asphaltene derivative (Type A), characterized by an aliphatic S-linkage, conforms to the molecular formula $C_{49}H_{55}NO_3S_2$, yielding an aggregate energy of 451.16 kcal/mol. Deconstructing this energetic profile reveals that torsional strain heavily dominates the system (426.76 kcal/mol), supplemented by subordinate contributions from bond stretching (11.33 kcal/mol), angular deformation (26.73 kcal/mol), van der Waals (vdW) forces (26.67 kcal/mol), and electrostatic pairings (-23.17 kcal/mol). The remaining energy terms contribute only minor fractions to the total energy.

For the optimized structure, the root mean square (RMS) force was 4.78×10^{-5} kcal/mol/Å, while the maximum force reached 2.44×10^{-4} kcal/mol/Å, indicating that the system is energetically stable.

Subsequent MD runs were executed over a 300 ps trajectory to observe the phase dynamics of the Type A derivative within an octane medium. Observations from these trajectories confirm a distinct propensity for these molecules to associate and eventually precipitate.

Within the scope of MD modeling, radial distribution functions (RDFs) serve as a standard metric for evaluating solute dissolution and inter-particle forces [31-33]. This mathematical tool maps the spatial probability of locating neighboring particles at specific radial distances from a central reference point. On the resulting plots, g(r) defines the relative local density of solvent species surrounding the central asphaltene, with g(r)max denoting the absolute highest concentration peak within that profile.

3. Results and Discussion

The model simulation boxes illustrating the aggregation of asphaltenes in a pure solvent environment are presented in Figures 3. To derive the corresponding solubility metrics, we configured a simulation cell at a baseline density to 0.6 g/cm³. Within this setup, a 78:22 mass ratio of solvent to solute, specifically comprising 250 octane entities and 10 asphaltene structures. Figure 3 captures the dynamic progression of these Type A structures within the aliphatic phase. The trajectory data confirms that these species progressively migrate toward one another, initiating cluster formation within the octane environment. This clustering phenomenon is primarily driven by the active functional moieties distributed across the asphaltene architectures and their resultant non-covalent interactions. Specifically, highly electronegative oxygen centers within the carboxyl segments draw in localized electropositive hydrogen sites, establishing robust H-bonding networks that tightly bind the molecules together. Ultimately, these bonding mechanisms act as the primary catalyst for the gross aggregation and phase separation of the asphaltene fraction in octane [34-38].

Beyond H-bonding networks, the overall intermolecular force profile is further reinforced by electrostatic (ES) and vdW forces. The magnitude of the vdW potential is largely determined by the solvent- accessible surface area of the species, along with its electron polarizability, which is directly governed by the total electron count and corresponding atomic radii. Conversely, the strength of the ES potential scales directly with the inherent polarity of the interacting chemical species.

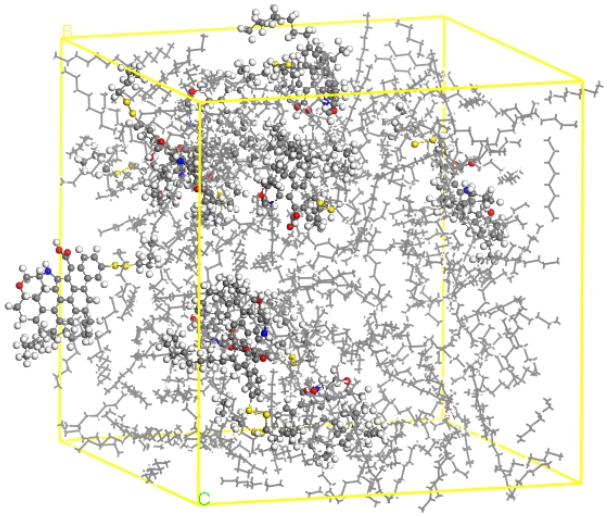

Figure 3. Configuration of the MD cell for the octane and asphaltene system. The environment incorporates 10 target asphaltene units and 250 solvent molecules, establishing a 78 to 22 mass percentage ratio of octane to the S branched asphaltene at a constant density of 0.6 g/cm^3.

A larger difference in electronegativity between atoms leads to a higher dipole moment. Consequently, incorporating heteroatomic species into the asphaltene architecture directly amplifies molecular polarity and reinforces the attractive forces across the system.

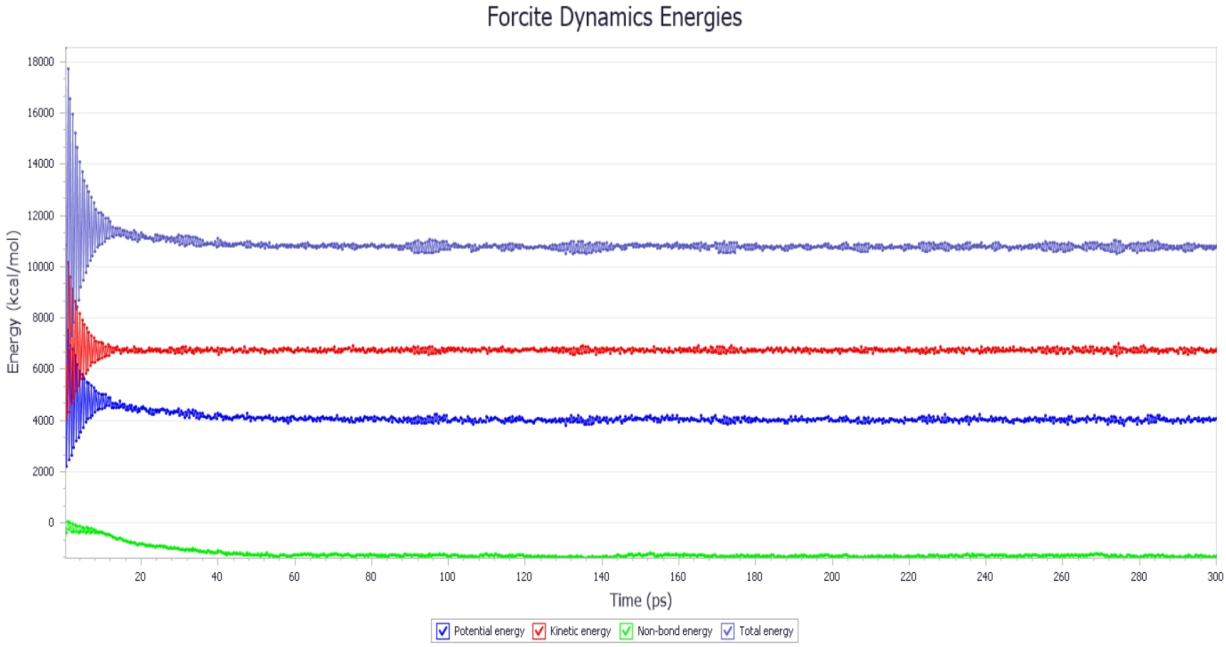

Figure 4. Molecular dynamics energy convergence for the system of octane/asphaltene S-branch during simulation running time of 300 picoseconds (ps) and timestep of 1 femtosecond (fs).

Energy fluctuations for the Type A asphaltene within the octane phase during the MD trajectory are plotted in Figure 4. The data demonstrate that total energy values exhibit negligible deviation throughout the 300 ps duration, validating the overall equilibrium of the modeled environment. In this context, the potential energy profile is primarily a manifestation of the interfacial forces between the asphaltene fraction and solvent species [39]. In the A structure, the –S-S– group located in the alkyl side chain influences molecular polarity and intermolecular interactions. Since octane is a low-polar solvent, electrostatic interactions are weak, while vdW interactions dominate the system [40-43].

Figure 5 presents the RDF of A asphaltene in octane. Utilizing RDF analysis allows for a detailed characterization of the attractive forces and the clustering propensity inherent to the asphaltene units. A specific count of 10 asphaltene structures and 250 octane molecules defined the composition of the simulation cell.

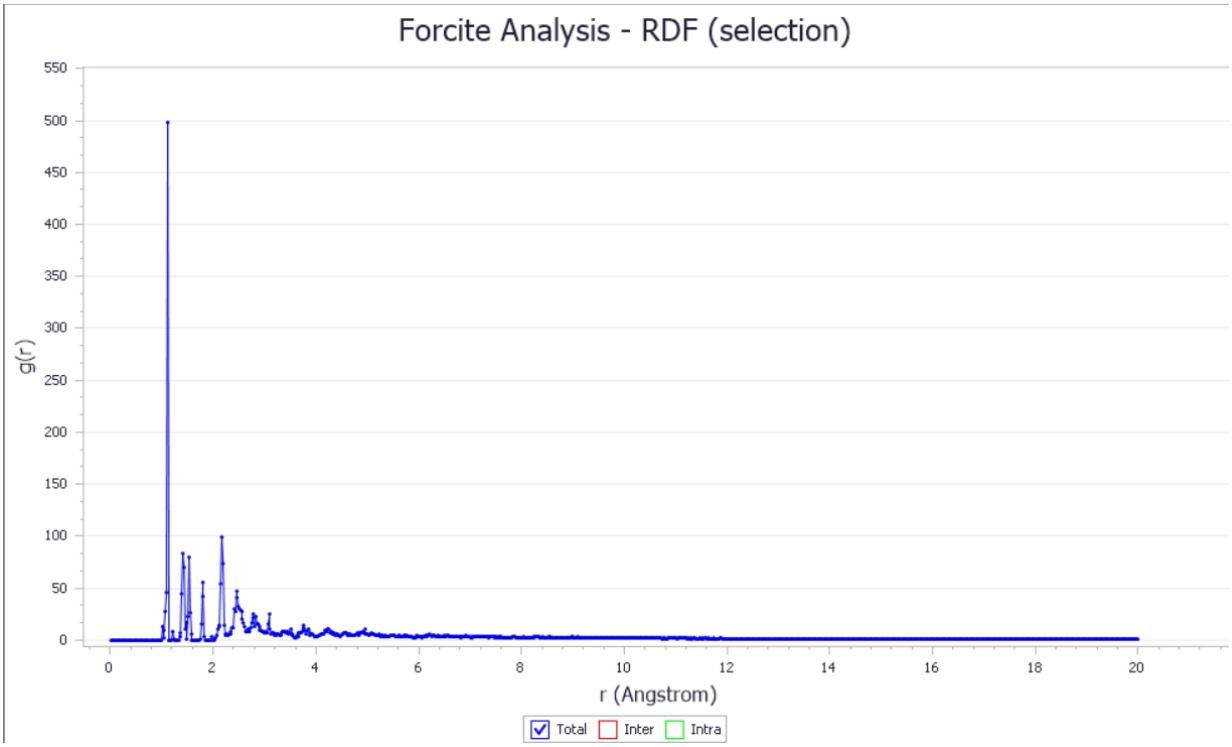

Figure 5. RDF profiles for the asphaltene/octane system extracted from the terminal 300 ps interval of the MD run. The computational box, which was assigned a mass- volume concentration of 0.6 g·cm^{-3}, encloses 10 asphaltene moieties together with 250 octane molecules, representing a 78:22 mass ratio of solvent to S-branched solute. Results were obtained using an NVT ensemble with a 1 fs time step under constant conditions of 298 K and 1 atm.

The RDF profiles for the analyzed system are illustrated in Figure 5. These curves exhibit five distinct peaks within the 1 to 2.5 Å interval, which signifies a predominant co-facial clustering of the asphaltene units. The dominant maximum originates from non- covalent π- overlap interactions among the polyaromatic cores, whereas the secondary peak identifies a T-shaped spatial orientation. This frontal-style association is largely governed by the synergy between polyaromatic cores and their surrounding side chains. Within this framework, the molecular units link via π-π interactions between aromatic rings alongside σ-σ interactions involving the aliphatic branches.

High RDF peak intensity indicates that the molecules aggregate more rapidly in the octane medium [44]. Since octane is a non-polar solvent, its interaction with asphaltene molecules is relatively weak, which facilitates molecular approach and aggregation [45]. The sharp peak observed at approximately 1 Å in the RDF curve suggests that the molecules come into close proximity, enhancing the aggregation process.

The clustering dynamics of asphaltenes are intrinsically linked to the topology of their aromatic cores and the inclusion of heteroatoms. The incorporation of N, O, and S constituents into the molecular architecture enhances asphaltene polarity [46]. However, the polarity of sulfur is lower than that of nitrogen and oxygen, making its effect relatively weaker. The highest molecular polarizability is observed in the aromatic core, which strengthens π-electron interactions and promotes aggregation [47-50]. Asphaltene molecules with large aromatic cores typically aggregate by adopting a coplanar stacked orientation.

To follow the temporal evolution of the Type A derivative's distribution in an octane, we conducted integrated RDF and radius of gyration (Rg) assessments. The Rg metric serves as a vital indicator for quantifying the spatial layout and structural density of molecular clusters in solution. MD outputs show that the Rg value initiated at approximately 0.6 ($r \approx 10$ Å), dropped to nearly 0.4 after a 150 ps duration, and remained stable until the 300 ps conclusion. This decrease indicates that the molecules approach each other and form more compact aggregates.

This behavior can be explained by the non-polar aliphatic nature of octane. Since octane interacts weakly with asphaltene molecules, the molecules tend to approach each other and aggregate. Clustering in this system is essentially propelled by π-π stacking between polyaromatic segments and vdW forces residing in the side-group regions. As a result, molecular compactness increases and the aggregation tendency becomes more pronounced.

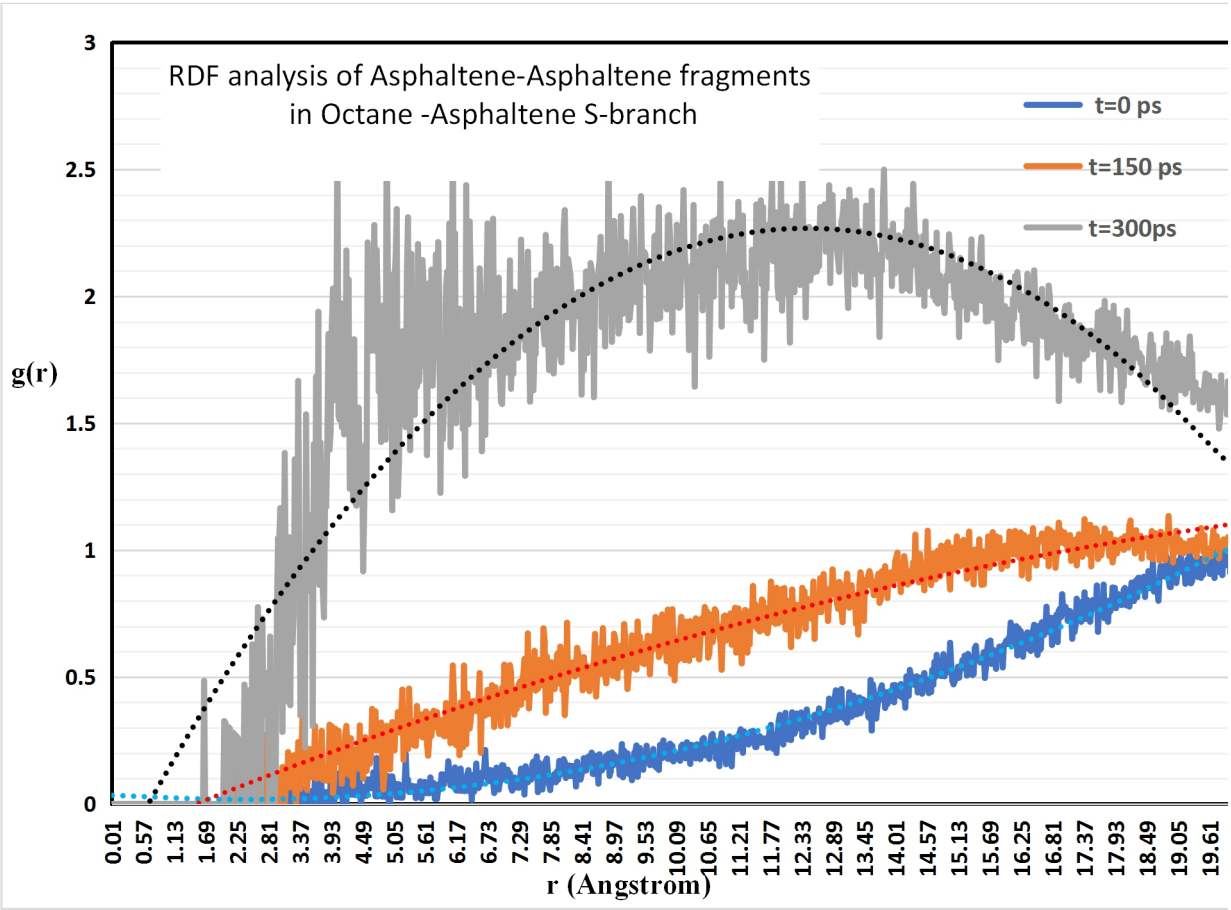

Figure 6. RDF profiles for asphaltene-asphaltene fragments in octane (S-branch type) at various time intervals. The MD cell, characterized by a density of 0.6 g/cm^3, incorporates 10 asphaltene units and 250 octane molecules, yielding a 78:22 mass ratio of solvent to solute. Data were collected at t = 0, 150, and 300 ps during a 300 ps trajectory using an NVT ensemble with a 1 fs time step under 298 K thermal condition and 1 atm pressure.

Figure 6 illustrates how the Type A asphaltene behaved in the MD trajectories within an octane environment. The trajectory reveals a progressive rise in the Rg parameter throughout the simulation. Initially, Rg was recorded at approximately 0.5, but escalated to roughly 2 at a separation $r \approx 19$ Å following 300 ps, signalling a sizeable increase in effective molecular volume.

These findings imply that the molecules transition into a more elongated conformation and increase their mutual separation. This trend stems from the non-polar, aliphatic character of octane,

which leads to minimal attractive forces between the solvent phase and the asphaltene structures. As a result, the molecular units favor a dispersed state instead of clustering into tight aggregates.

The increase in the Rg value is also associated with enhanced molecular mobility within the system, leading to greater intermolecular distances and a more expanded configuration. This behavior may contribute to a reduced tendency for asphaltene precipitation, which is important for understanding and potentially mitigating deposition problems in petroleum systems.

The kinetics of clustering and solubility variations are governed by the interplay between asphaltene architecture and the specific properties of the surrounding solvent. Over the observed timeframe, the Type A variant maintains a higher degree of stability and remains uniformly distributed within the phase.

Such insights are vital for deciphering the phase dynamics of asphaltenes within complex petroleum matrices. The enhanced dissolution of the Type A structure in octane could potentially mitigate operational hurdles, specifically regarding flow assurance issues like pipeline fouling and solid dropout. MD outputs confirm that the Type A species, which incorporates S within its aliphatic side-group, demonstrates superior phase stability and dispersion in octane relative to alternative structural motifs. This characteristic is fundamentally linked to the molecular topology and the resulting solute-solvent forces, both of which serve as primary determinants for the behavior of these complex macromolecules in a dissolved state.

4. Conclusions

The performed MD runs provide a detailed account of the Type A asphaltene dynamics within an aliphatic octane environment. The RDF and radius of gyration analyses indicate that the increase in Rg during the simulation corresponds to a more dispersed molecular arrangement. This behavior is associated with the non-polar nature of octane and its relatively weak interaction with asphaltene molecules. As a result, a asphaltene shows a tendency toward dispersion rather than aggregation in octane.

These observations offer significant practical value for managing asphaltene stability, especially in optimizing strategies to inhibit deposition throughout the extraction and transit stages of the petroleum value chain.

References

[1] Khuduzade A.I., Abbasov O.R., Guliyev I.S. et al. Geochemical-paleontological study of Mesozoic source rocks, Eurasian–Gondwana junction, 2026, Azerbaijan. *Episodes* (2026). https://doi.org/10.18814/epiiugs/2026/026002

[2] Aliyev A.A., Abbasov O.R., Ibadzade A.J., Mammadova A.N. Genesis and organic geochemical characteristics of oil shale in Eastern Azerbaijan. *SOCAR Proceedings* 3 (2018) 4–15. https://doi.org/10.5510/OGP20180300356

[3] Arab D., Kantzas A., Bryant S.L. Nanoparticle stabilized oil-in-water emulsions: A critical review. *J. Pet. Sci. Eng.* 163 (2018) 217–242. https://doi.org/10.1016/j.petrol.2017.12.091

[4] Aliyev A.A., Abbasov O.R. Distribution patterns, organic geochemistry and mineralogy of oil shales in Azerbaijan. *Gornyi Zhurnal* (8) (2020) 13–18. https://doi.org/10.17580/gzh.2020.08.02

[5] Aliyev A.A., Abbasov O.R. Mineralogical and geochemical proxies for Middle Eocene oil shales… *Mineralia Slovaca* 51(2) (2019) 157–174.

[6] Abbasov V.M. et al. Use of ultrasonic pretreatment in aerobic oxidation of paraffin hydrocarbons. *Iranian J. Chem. Chem. Eng.* 43(2) (2024) 707–713. https://doi.org/10.30492/IJCCE.2023.1971436.5685

[7] Aliyev A.A. et al. Mineralogy, geochemistry and paleoweathering of oil shales in Azerbaijan. *SOCAR Proceedings* 1 (2022) 24–36. https://doi.org/10.5510/OGP20220100625

[8] Aliyev A.A., Abbasov O.R. Provenance and tectonic setting of oil shale… *Geodynamics* 1(26) (2019) 43–59. https://doi.org/10.23939/jgd2019.01.043
[9] Aliyev A. et al. Mineralogy and geochemistry of oil shale in Azerbaijan. *Visnyk V.N. Karazin Univ.* 50 (2019) 11–26. https://doi.org/10.26565/2410-7360-2019-50-01
[10] Branco V.M. et al. Asphaltene flocculation and collapse from petroleum fluids. *J. Pet. Sci. Eng.* 32(2) (2001) 217–230. https://doi.org/10.1016/S0920-4105(01)00163-2
[11] Mullins O.C. The asphaltenes. *Annu. Rev. Anal. Chem.* 4 (2011) 393–418. https://doi.org/10.1146/annurev-anchem-061010-113849
[12] Langevin D., Argillier J.F. Interfacial behavior of asphaltenes. *Adv. Colloid Interface Sci.* 233 (2016) 83–93. https://doi.org/10.1016/j.cis.2015.10.005
[13] Abdullayev Y. et al. Construction of azo-group containing polycyclic imidazole derivatives. *ChemistrySelect* 5 (2020) 6224–6229. https://doi.org/10.1002/slct.202000949
[14] Gray M.R. et al. Supramolecular assembly model for asphaltene aggregation. *Energy Fuels* 25 (2011) 3125–3134. https://doi.org/10.1021/ef200654p
[15] Mullins O.C., Zare R.N. Laser-based mass spectrometric assessment of asphaltenes. *Energy Fuels* 29 (2015) 2833–2842. https://doi.org/10.1021/ef5020764
[16] Biktagirov T. et al. Vanadyl porphyrins in crude oil by ENDR spectroscopy. *Energy Fuels* 31 (2017) 1243–1249. https://doi.org/10.1021/acs.energyfuels.6b02494
[17] Yolchuyeva U. et al. Surakhani crude oil compounds study. *J. Pet. Explor. Prod. Technol.* 14 (2024) 289–302. https://doi.org/10.1007/s13202-023-01702-6
[18] Ghosh A.K. et al. Review on aggregation of asphaltenes. *Fuel* 185 (2016) 541–554. https://doi.org/10.1016/j.fuel.2016.08.031
[19] Hemmati-Sarapardeh A. et al. Asphaltene aggregation in toluene. *J. Mol. Liq.* 264 (2018) 410–424. https://doi.org/10.1016/j.molliq.2018.04.061
[20] Seidova S.A. et al. Ionic liquid extraction in dearomatization. *SOCAR Proceedings* 3 (2024) 107–112.
[21] Guo W. et al. Nanoscale asperities plasticity. *Nano Lett.* 15 (2015) 6582–6585. https://doi.org/10.1021/acs.nanolett.5b02306
[22] Chen Z.T. et al. Molecular structure of petroleum asphaltene. *Struct. Bond.* 168 (2016) 1–38. https://doi.org/10.1007/4302015181
[23] Yolchuyeva U. et al. Photochemical conversion in Balakhani oil. *J. Pet. Sci. Eng.* 196 (2021) 108089. https://doi.org/10.1016/j.petrol.2020.108089
[24] Wang K.R. et al. Molecular aggregation behavior of cyclodextrins. *J. Phys. Chem. B* 114 (2010) 101–106. https://doi.org/10.1021/jp908699b
[25] Yolchuyeva U. et al. Photochemical investigation of crude oil aromatics. *Appl. Petrochem. Res.* 10 (2020) 139–148. https://doi.org/10.1007/s13203-020-00253-9
[26] Seidova S.A. Extraction methods of motor fuel cleaning. *ChemChemTech* 62 (2019) 30–39.
[27] Ibrahimova M.J. et al. Ionic-liquid extraction of kerosene fraction. *Chem. Probl.* 17 (2019) 576–583.
[28] Baram J. et al. Self-assembly via reversible charging. *J. Am. Chem. Soc.* 130 (2008) 14966–14967. https://doi.org/10.1021/ja807027w
[29] Zhang X. et al. Perylene dye nanocapsules. *Nat. Chem.* 1 (2009) 623–629. https://doi.org/10.1038/nchem.368
[30] Mammadov A.M. et al. Phenanthroimidazole derivatives study. *Bull. Russ. Acad. Sci.: Phys.* 89(9) (2025) 1619–1625. https://doi.org/10.1134/S1062873825712322
[31] Yolchuyeva U. et al. Asphaltene dispersion surfactant study. *Fuel* 404 (2026) 136286. https://doi.org/10.1016/j.fuel.2025.136286
[32] Seyyedattar M. et al. Molecular dynamics in reservoir analysis. *Earth-Sci. Rev.* 192 (2019) 194–213. https://doi.org/10.1016/j.earscirev.2019.02.019
[33] Aray Y. et al. Asphaltene solubility simulation. *J. Phys. Chem. A* 115 (2011) 11495–11507. https://doi.org/10.1021/jp204319n

[34] Yolchuyeva U. et al. Sulfur heteroatoms in asphaltenes. *J. Mol. Model.* 31 (2025) 133. https://doi.org/10.1007/s00894-025-06358-z
[35] Jafarova R.A. et al. Phototransformation of oil sands bitumen. *Coke Chem.* 68 (2025) 45–51. https://doi.org/10.3103/S1068364X25600022
[36] Jafarova R.A. et al. Thermo-oxidation processes in petroleum. *Pet. Process. Petrochem.* 26(1) (2025) 240–255. https://doi.org/10.62972/1726-4685.2025.1.240
[37] Jafarova R.A. et al. Photooxidation of petroleum aromatics. *J. Appl. Spectrosc.* 91(2) (2024) 357. https://doi.org/10.1007/s10812-024-01728-6
[38] Yolchuyeva U. et al. Asphaltene structure of Azerbaijani crude oil. *Fuel* 373 (2024) 132084. https://doi.org/10.1016/j.fuel.2024.132084
[39] Mammadhasanov K.K. et al. Ionic-liquid extraction simulation. *Mod. Phys. Lett. B* 37(30) (2023) 2350139.
[40] Ibragimova M.J. et al. Ionic liquids in diesel fuel purification. *Azerbaijan Chem. J.* 3 (2024) 20–28.
[41] Ibragimova M.D. et al. Aromatic hydrocarbons in diesel fuel. *SOCAR Proceedings* 3 (2022) 101–105.
[42] Farzaliyev V.M. et al. Lubricant oil additives synthesis. *Chem. Probl.* 21(1) (2023) 48–56.
[43] Haji-Akbari N. et al. Asphaltene aggregation model. *Energy Fuels* 27 (2013) 2497–2505. https://doi.org/10.1021/ef4001665
[44] Ibrahimova M.J. et al. Microbial corrosion study. *Chem. Probl.* 23(3) (2025) 407–413.
[45] Yolchuyeva U. et al. Surakhani oil GC-MS study. *Pet. Process. Petrochem.* 23(3) (2022) 436–445.
[46] Abbasov O.R. et al. Oil-generating potential of Eocene shales. *Boletín Soc. Geol. Mex.* 77(1) (2025). https://doi.org/10.18268/bsgm2025v77n1a020724
[47] Sengupta S. et al. Polyelectrolyte membrane simulation. *Int. J. Hydrogen Energy* 42 (2017) 27254–27268. https://doi.org/10.1016/j.ijhydene.2017.09.078
[48] Tang X. et al. Surfactant flooding simulation. *J. Phys. Chem. B* 123 (2019) 277–288. https://doi.org/10.1021/acs.jpcb.8b09777
[49] Gamba M. et al. Montmorillonite interaction study. *Appl. Clay Sci.* 137 (2017) 59–68. https://doi.org/10.1016/j.clay.2016.12.001
[50] Samieadel A. et al. Wax effect in asphalt binder. *Constr. Build. Mater.* 157 (2017) 1163–1172. https://doi.org/10.1016/j.conbuildmat.2017.09.188